
TOMA: Topological Map Abstraction for Reinforcement Learning

Zhao-Heng Yin, Wu-Jun Li

National Key Laboratory for Novel Software Technology
Department of Computer Science and Technology
Nanjing University, Nanjing 210023, China
zhaohengyin@gmail.com, liwujun@nju.edu.cn

Abstract

Animals are able to discover the topological map (graph) of surrounding environment, which will be used for navigation. Inspired by this biological phenomenon, researchers have recently proposed to generate graph representation for Markov decision process (MDP) and use such graphs for planning in reinforcement learning (RL). However, existing graph generation methods suffer from many drawbacks. One drawback is that existing methods do not learn an abstraction for graphs, which results in high memory and computation cost. This drawback also makes generated graph non-robust, which degrades the planning performance. Another drawback is that existing methods cannot be used for facilitating exploration which is important in RL. In this paper, we propose a new method, called *topological map abstraction* (TOMA), for graph generation. TOMA can generate an abstract graph representation for MDP, which costs much less memory and computation cost than existing methods. Furthermore, TOMA can be used for facilitating exploration. In particular, we propose *planning to explore*, in which TOMA is used to accelerate exploration by guiding the agent towards unexplored states. A novel experience replay module called *vertex memory* is also proposed to improve exploration performance. Experimental results show that TOMA can outperform existing methods to achieve the state-of-the-art performance.

1 Introduction

Animals are able to discover topological map (graph) of surrounding environment [O’Keefe and Dostrovsky, 1971, Moser et al., 2008], which will be used as hints for navigation. For example, previous maze experiments on rats [O’Keefe and Dostrovsky, 1971] reveal that rats can create mental representation of the maze and use such representation to reach the food placed in the maze. In cognitive science society, researchers summarize these discoveries in *cognitive map theory* [Tolman, 1948], which states that animals can extract and code the structure of environment in a compact and abstract map representation.

Inspired by such biological phenomenon, researchers have recently proposed to learn (generate) topological graph representation for Markov decision process (MDP) and use such graphs for planning in reinforcement learning (RL). To generate graphs, existing methods generally treat the states in a replay buffer as vertices. For the edges of the graphs, some methods like SPTM [Savinov et al., 2018] train a reachability predictor via self-supervised learning and combine it with human experience to construct the edges. Other methods like SoRB [Eysenbach et al., 2019] exploit a goal-conditioned agent to estimate the distance between vertices, based on which edges are constructed. These existing methods suffer from the following drawbacks. Firstly, these methods do not learn an abstraction for graphs and usually consider all the states in the buffer as vertices [Savinov et al., 2018], which results in high memory and computation cost. This drawback also makes generated graph non-robust, which will degrade the planning performance. Secondly, existing methods cannot be used for facilitating

Preprint.

exploration, which is important in RL. In particular, methods like SPTM [Savinov et al., 2018] rely on human sampled trajectories to generate the graph, which is infeasible in RL exploration. Methods like SoRB [Eysenbach et al., 2019] require training another goal-conditioned agent. Such training procedure assumes knowledge of the environment since it requires to generate several goal-reaching tasks to train the agent. This practice is also intractable in RL exploration.

In this paper, we propose a new method, called TOPological Map Abstraction (TOMA), for graph generation. The main contributions of this paper are outlined as follows:

- TOMA can generate an abstract graph representation for MDP. Different from existing methods in which each vertex of the graph represents a state, each vertex in TOMA represents a cluster of states. As a result, compared with existing methods TOMA has much less memory and computation cost, and can generate more robust graph for planning.
- TOMA can be used to facilitate exploration. In particular, we propose *planning to explore*, in which TOMA is used to accelerate exploration by guiding the agent towards unexplored states. A novel experience replay module called *vertex memory* is also proposed to improve exploration performance.
- Experimental results show that TOMA can robustly generate abstract graph representation on several 2D world environments with different types of observation and can outperform previous baseline methods to achieve the state-of-the-art performance.

2 Algorithm

2.1 Notations

In this paper, we model a RL problem as a Markov decision process (MDP). A MDP is a tuple $M(S, A, R, \gamma, P)$, where S is the state space, A is the action space, $R : S \times A \rightarrow \mathbb{R}$ is a reward function, γ is a discount factor and $P(s_{t+1}|s_t, a_t)$ is the transition dynamic. $\rho(x, y) = \|x - y\|_2$ denotes Euclidean distance. $G(V, E)$ denotes a graph, where V is its vertex set and E is its edge set. For any set X , we define its indicator function $\mathbb{1}_X(x)$ as follows: $\mathbb{1}_X(x) = 1$ if $x \in X$, $\mathbb{1}_X(x) = 0$ if $x \notin X$.

2.2 TOMA

Figure 1 gives an illustration of TOMA, which tries to map states to an abstract graph. A landmark set L is a subset of S and each landmark $l_i \in L$ is a one-to-one correspondence to a vertex v_i in the graph. Each l_i and v_i will represent a cluster of states. In order to decide which vertex a state $s \in S$ corresponds to, we first use a locality sensitive embedding function ϕ_θ to calculate its latent representation $z = \phi_\theta(s)$ in the embedding space Z . Then if z 's nearest neighbor in the embedded landmark set $\phi_\theta(L) = \{\phi_\theta(l) | l \in L\}$ is $\phi_\theta(l_i)$, we will map s to vertex $v_i \in V$.

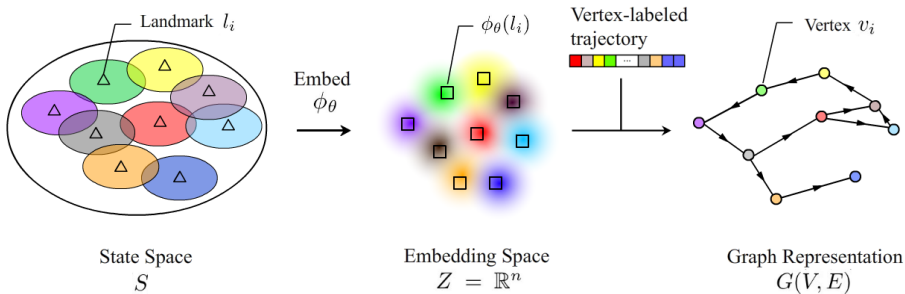


Figure 1: Illustration of TOMA. We will pick up some states as landmarks (colored triangles) in the state space of the original MDP M . Each landmark l_i is a one-to-one correspondence to a vertex v_i (colored circles) in graph G and covers some areas in S . Embedding ϕ_θ is trained by self-supervised learning. We will label each state on a trajectory with a corresponding vertex and use it to generate the graph dynamically.

2.2.1 Locality Sensitive Embedding

A locality sensitive embedding is a local distance preserving mapping ϕ_θ from state space S to an embedding space Z , which is an Euclidean space \mathbb{R}^n in our implementation. Given a trajectory $T = (s_0, a_0, s_1, a_1, \dots, s_n)$, we can use $d_{ij} = |j - i|/r$ to estimate the distance between s_i and s_j . Here r is a radius hyper-parameter to re-scale the distance and we will further explain its meaning later. In practice, however, d_{ij} is a noisy estimation for shortest distance and approximating it directly won't converge in most cases. Hence, we propose to estimate which interval the real distance lies in. First, we define three indicator functions:

$$\chi_1(x) = \mathbb{1}_{[0,1]}(x), \quad (1)$$

$$\chi_2(x) = \mathbb{1}_{(1,3]}(x), \quad (2)$$

$$\chi_3(x) = \mathbb{1}_{(3,+\infty)}(x), \quad (3)$$

which mark three disjoint regions $[0, 1]$, $(1, 3]$, $(3, +\infty)$, respectively. Then we define an anti-bump function $\xi_{a,b}(x) = \text{Relu}(-x + a) + \text{Relu}(x - b)$. Here, $\text{Relu}(x) = \max(0, x)$ is the rectified linear unit (ReLU) function [Glorot et al., 2011]. With this $\xi(x)$, we can measure the deviation from the above intervals. Let

$$\mathcal{L}_1(x) = \xi_{-\infty,1}(x) = \text{Relu}(x - 1), \quad (4)$$

$$\mathcal{L}_2(x) = \xi_{1,3}(x) = \text{Relu}(-x + 1) + \text{Relu}(x - 3), \quad (5)$$

$$\mathcal{L}_3(x) = \xi_{3,+\infty}(x) = \text{Relu}(-x + 3), \quad (6)$$

and let $d'_{ij} = \rho(\phi_\theta(s_i), \phi_\theta(s_j))$ denote the distance between s_i and s_j in the embedding space. Our embedding loss is defined as

$$\mathcal{L}(\theta) = \mathbb{E}_{(s_i, s_j) \sim P_s} (\chi_1(d_{ij})\mathcal{L}_1(d'_{ij}) + \lambda_1\chi_2(d_{ij})\mathcal{L}_2(d'_{ij}) + \lambda_2\chi_3(d_{ij})\mathcal{L}_3(d'_{ij})). \quad (7)$$

Here P_s is a sample distribution which will be described later, λ_1 and λ_2 are two hyper-parameters to balance the importance of the estimation for different distances. We find that a good choice is to pick $\lambda_1 = 0.5$, $\lambda_2 = 0.2$ to ensure that our model focuses on the terms with lower variance. In this equation, there are some critical components to notice:

Radius r As we will see later, the hyper-parameter r will determine the granularity of each graph vertex, which we term as radius. If we define the k -ball neighborhood of $s \in S$ to be

$$B_k(s) = \{s' \in S | \rho(\phi_\theta(s'), \phi_\theta(s)) < k\}, \quad (8)$$

then $B_k(s)$ will cover more states when r is larger. During the graph generation process, we will remove redundant vertices by checking whether $B_1(l_i)$ and $B_1(l_j)$ intersect too much. Re-scaling by r makes it easier to train the embedding function.

Sample Distribution P_s The state pair (s_i, s_j) in the loss function is sampled from a neighborhood biased distribution P_s . We will sample (s_i, s_j) ($i < j$) with probability α , if $j - i \leq 4r$. And we will sample (s_i, s_j) ($i < j$) with probability $1 - \alpha$, if $j - i > 4r$. We simply take $\alpha = 0.5$ and the choice of α is not sensitive in our experiment. In the implementation, we use this sample distribution to draw samples from trajectory and put them into a replay pool. Then we train the embedding function by uniformly drawing samples from the pool.

Anti-Bump Functions The idea of anti-bump function is inspired by the *partition of unity theorem* in differential topology [Hirsch, 1997], where a bunch of bump functions are used to glue the local charts of manifold together so as to derive global properties of differential manifolds. In proofs of many differential topology theorems, one crucial step is to use bump function to segregate each local chart into three disjoint regions by radius 1, 2 and 3, which is analogous to our method. The loss function is crucial in our method, as in experiment we find that training won't converge if we replace this loss function with a commonly used L_2 loss.

2.2.2 Dynamic Graph Generation

An abstract graph representation $G(V, E)$ should satisfy the following basic requirements:

- *Simple*: For any $v_i, v_j \in V$, if $v_i \neq v_j$, $B_1(l_i) \cap B_1(l_j)$ should not contain too many elements.

- *Accurate*: For any $v_i, v_j \in V$ and $v_i \neq v_j$, $\langle v_i, v_j \rangle \in E$ if and only if the agent can travel from some $s \in B_1(l_i)$ to some $s' \in B_1(l_j)$ in a small number of steps.
- *Abundant*: $\cup_{i: v_i \in V} B_1(l_i)$ should cover the states as many as possible.
- *Dynamic*: G grows dynamically, by absorbing topology information of novel states.

In the following content, we show a dynamic graph generation method fulfilling such requirements. First, we introduce the basic operations in our generation procedure. The operations can be reduced to the following three categories:

Initializing

[I1: Initialize] If $V = \emptyset$, we will pick a landmark from currently sampled trajectories and add a vertex into V accordingly. In our implementation, this landmark is the initial state of the agent.

Adding

[A1: Add Labels] For each state s on a trajectory, we label it with its corresponding graph vertex. Let $i = \arg \min_{j: v_j \in V} \rho(\phi_\theta(s), \phi_\theta(l_j))$ and $d = \rho(\phi_\theta(s), \phi_\theta(l_i))$. There are three possible cases: (1) $d \in [0, 1.5]$. We label s with v_i . (2) $d \in [2, 3]$. We consider s as an appropriate landmark candidate. Therefore, we label s with NULL but add it to a candidate queue. (3) Otherwise, s is simply labelled with NULL.

[A2: Add Vertices] We move some states from the candidate queue into the landmark set and update V accordingly. Once a state is added to the landmark set, we will relabel it from NULL to its vertex identifier.

[A3 Add Edges] Let the labelled trajectory to be $(v_{i_0}, v_{i_1}, \dots, v_{i_n})$. If we find v_{i_k} and $v_{i_{k+1}}$ are different vertices in the existing graph, we will add an edge $\langle v_{i_k}, v_{i_{k+1}} \rangle$ into the graph.

Checking

[C1: Check Vertices] If $\rho(\phi_\theta(l_i), \phi_\theta(l_j)) < 1.5$, then we will merge v_i and v_j .

[C2: Check Edges] For any edge $\langle v_i, v_j \rangle$, if $\rho(\phi_\theta(l_i), \phi_\theta(l_j)) > 3$, we will remove this edge.

For efficient nearest neighbor search, we use Kd-tree [Bentley, 1975] to manage the vertices. Based on the above operations, we can get our graph generation algorithm TOMA which is summarized in Algorithm 1.

Algorithm 1 Topological Map Abstraction (TOMA)

- 1: Pool $P \leftarrow \emptyset$. Vertex set $V \leftarrow \emptyset$. Edge set $E \leftarrow \emptyset$. Graph $G(V, E)$.
 - 2: **for** $t = 1, 2, \dots$ **do**
 - 3: Sample a trajectory T using some policy π or by random.
 - 4: Sample state pairs from T using distribution P_s and put them to P .
 - 5: Training the embedding function ϕ_θ using samples from P .
 - 6: Initialize G using (I1) if it's empty.
 - 7: Add vertices and edges using (A1) to (A3).
 - 8: Check the graph using (C1) to (C2).
 - 9: **end for**
-

2.2.3 Increasing Robustness

In practice, we find TOMA sometimes provides inaccurate estimation on image domains without rich visual information. This is similar to the findings of [Eysenbach et al., 2019], which uses an ensemble of distributional value function for robust distance estimation. To increase robustness, we can also use an ensemble of embedding functions to provide reliable neighborhood relationship estimation on these difficult domains. The functions in the ensemble are trained with data drawn from the same pool. During labelling, each function will vote a nearest neighbor for the given observation and TOMA will select the winner as the label. To evaluate the distance between states, we use the average of the distance estimation of all embedding functions. In [Eysenbach et al., 2019], the authors find that ensemble is an indispensable component in their value function based method for all applications. On the contrary, TOMA does not require ensemble to increase robustness on applications with rich information.

2.3 Planning to Explore

Since the graph of TOMA expands dynamically as agent samples in the environment, it can be fitted into standard RL settings to facilitate exploration. We choose the furthest vertex or the least visited vertex as the ultimate goal for agent in each episode. During sampling we periodically run Dijkstra’s algorithm to figure out the path towards the goal from the current state, and the vertices on the path are used as intermediate goals. To ensure that the agent can stably reach the border, we further introduce the following memory module.

Vertex Memory We observe that the agent usually fails to explore efficiently simply because it forgets how to reach the border of explored area as training goes on. In order to make agent recall the way to the border, we require that each vertex v_i should maintain a small replay buffer to record successful transitions into the cluster of v_i . Then, if our agent is going towards goal g and the vertices on the shortest path towards the corresponding landmark of g are v_1, v_2, \dots, v_k , then we will draw some experience from the replay pool of v_1, v_2, \dots, v_k to inform the agent of relevant knowledge during training. In the implementation, we use the following replay strategy: half of the training data are drawn from experience of vertex memory which provides task-specific knowledge, while the other half are drawn from normal hindsight experience replay (HER) [Andrychowicz et al., 2017] which provides general knowledge. We will use the sampled trajectory to update the memory of visited vertices at the end of each epoch. The overall procedure is summarized in Algorithm 2.

Algorithm 2 Planning to Explore with TOMA

- 1: **for** $t = 1, 2, \dots$ **do**
 - 2: Set a goal g using some criterion.
 - 3: Sample a trajectory T under the guidance of intermediate goals.
 - 4: Update graph using T (Algorithm 1).
 - 5: Update vertex memory and HER using T .
 - 6: Train the policy π using experience drawn from vertex memory and HER.
 - 7: **end for**
-

3 Experiments

In the experiments, we first show that TOMA can generate abstract graphs via visualization and demonstrate that such graph is suitable for planning. Then we carry out exploration experiment in some sparse reward environments and show that TOMA can facilitate exploration.

3.1 Graph Generation

3.1.1 Visualization

In this section, we test whether TOMA can generate abstract graph via visualization. In order to provide intuitive visualization, we use several 2D world environments to test TOMA, which are shown in Figure 2(a). In this planar world, there are some walls which agent can not cross through. The agent can take 4 different actions at each step: going up, down, left or right for one unit distance. To simulate various reinforcement learning domains, we test the agent on four different types of observation respectively: sensor, noisy sensor, MNIST digit [LeCun and Cortes, 2010] and top-down observation. Sensor observation is simply the (x, y) coordinates of the agent and the noisy sensor observation is the coordinates with 8 random features. Both MNIST digit and top-down observation are image observations. MNIST digit observation is a mixture of MNIST digit images, which is similar to the reconstructed MNIST digit image of variational auto-encoders [Kingma and Welling, 2014]. The observed digit is based on the agent’s position and varies continuously as agent moves in this world. Top-down observation is a blank image with a white dot indicating the agent’s location. We use three different maps: “Empty”, “Lines” and “Four rooms”. Since in this experiment we only care about whether TOMA can generate abstract graph representation from enough samples, we spawn a random agent at a random position in the map at the beginning of each episode. Each episode lasts 1000 steps and we run 500 episodes in each experiment. We use ensemble to increase robustness only for the top-down observation. The visualization result of the graph is provided in the Figure 2(b). Despite very few missing edges or wrong edges, the generated graphs are reasonable in

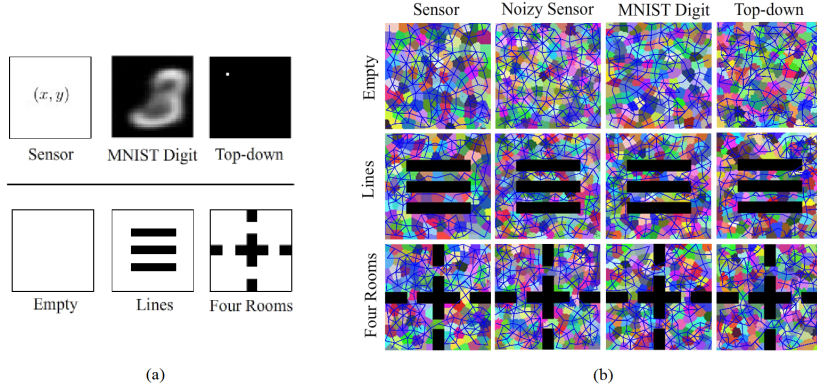


Figure 2: (a) 2D world observations (above) and maps (below). (b) The generated graph of different 2D world environments under different types of observation. Each connected colored segment indicates a vertex with its state coverage. The blue line connecting two segments denotes an edge connecting the corresponding two vertices.

Table 1: Performance of different graph generation algorithms

Algorithm	Sensor			MNIST Digit			Top-down		
	Suc.	Size	Time	Suc.	Size	Time	Suc.	Size	Time
SPTM	73.4%	10k	> 1s	60.3%	10k	> 1s	61.5%	10k	> 1s
SoRB	77.6%	1k	> 0.5s	56.3%	1k	> 0.5s	52.0%	1k	> 0.5s
TOMA	87.5%	0.1k	< 0.1s	77.2%	0.1k	< 0.1s	75.3%	0.1k	< 0.1s

nine cases. The successful result on various observation domains suggest that TOMA is a reliable and robust abstract graph generation algorithm.

3.1.2 Planning Performance

In this experiment, we first pretrain a goal-conditioned agent which can reach nearby goals. Then we use the generated graph of TOMA in Section 3.1.1 and recent baselines including SPTM and SoRB to plan for agent respectively. We randomly generate goal-reaching tasks in Four Rooms on three different types of observation. Table 1 shows the average success rate of navigation, the size of the generated graph and the planning time. The agent using the graph of TOMA has a higher success rate in navigation. The main reason behind this is that the generated graph of TOMA can capture more robust topological structure. SPTM and SoRB maintain too many vertices and as a result, we find that they usually miss neighborhood edges or introduce false edges since the learned model is not accurate on all the vertex pairs. Moreover, TOMA also consumes less memory and plans faster compared with other methods. To localize the agent, TOMA only needs to call the embedding network once, and uses the efficient nearest neighbor search to find out the corresponding vertex in $O(\log |V|)$ time. Since TOMA maintains less vertices and edges, the Dijkstra algorithm applied in planning also returns the shortest path faster. The efficiency of planning is crucial since it significantly reduces the training time of Algorithm 2, which requires iterative planning during online sampling.

3.2 Unsupervised Exploration

3.2.1 Setting

In this section, we test whether Algorithm 2 can explore the sparse-reward environments. The environments for test are MountainCar and another 2D world called Snake maze, which are shown in Figure 3. MountainCar is a classical RL experiment where the agent tries to drive a car up to the hill on the right. Snake maze is a 2D world environment where the agent tries to go from the upper-left corner to the bottom-right corner. In this environment, reaching the end of the maze usually requires 300-400 steps. This is a challenging task since the agent should learn how to make turns at the right points in a long distance travel.

In these environments, we set the reward provided by environment to 0. We use DQN [Mnih et al., 2015] as the agent for MountainCar and Snake maze as they are tasks with discrete actions. In MountainCar, we set the goal of each episode to be the least visited landmark since the agent needs to explore an acceleration skill and the furthest vertex will sometimes guide the agent into a local minima. In Snake maze, we simply set the goal to be the furthest vertex in the graph. Since HER makes up part of our memory, we use DQN with HER as the baseline for comparison. We test two variants of TOMA: TOMA with vertex memory (TOMA-VM) and TOMA without vertex memory (TOMA). For fair comparison, these three methods share the same DQN and HER parameters. For MountainCar, we train the agent for 20 iterations and each iteration lasts for 200 steps. For Snake maze on sensor observation, we train the agent for 300 iterations. For Snake maze on MNIST digit and top-down observation, we train the agent for 500 iterations. Each iteration lasts for 1000 steps. In each iteration, we record the max distance the agent reached in the past history. We additionally calculate a mean reached distance for experiments in Snake maze, which is the average reached distance in the past 10 iterations. We repeat the experiments for 5 times, and report the mean results.

3.2.2 Result

The results are shown in Figure 5. We can find that TOMA-VM and TOMA outperform the baseline HER in all these experiments. In MountainCar experiment, we find that the HER agent fails to discover the acceleration skill and gets stuck at the local minima. In contrast, both TOMA-VM and TOMA agents can discover the acceleration skill within 3 iterations and successfully climb up to the right hill. Figure 4 (a) shows some intermediate goals of the agent of TOMA-VM, which intuitively demonstrates the effectiveness of TOMA-VM. In Snake maze with sensor observation, the HER agent cannot learn any meaningful action while our TOMA-VM agent can successfully reach the end of the maze. Though the TOMA agent cannot always successfully reach the border of the exploration states in every iteration, there is still over 50% probability of reaching the final goal. In the image based experiments, however, we find that the learning process of goal-conditioned DQN on such a domain is not stable enough. Therefore, our agent can only reach the left or middle bottom corner of the maze on average.

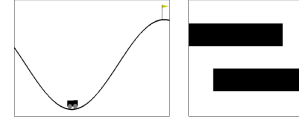


Figure 3: Environments used to test the exploration performance. (Left) Mountain car. (Right) Snake maze.

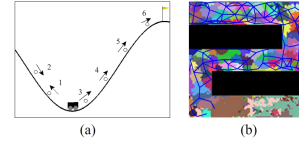


Figure 4: (a) Intermediate goals in MountainCar. (b) The generated graph in top-down Snake maze during exploration.

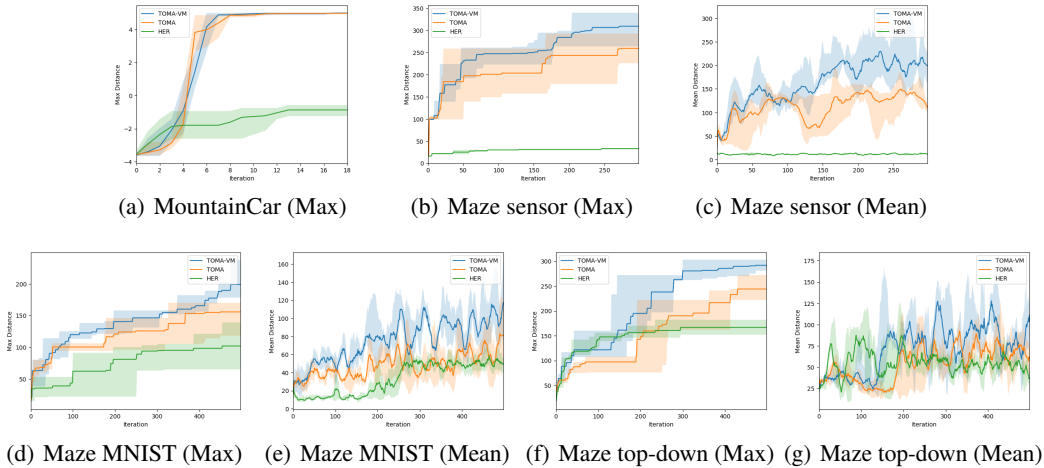


Figure 5: Reached distance of TOMA-VM, TOMA and HER. We also plot the mean of the reached distance for Snake maze experiments. TOMA-VM consistently performs better than the baseline method HER which gets stuck at local minima due to the lack of graph guidance.

A typical example of the generated graph representation during exploration in Top-down Snake maze is shown in Figure 4 (b). This generated graph does provide correct guidance, but the agent struggles to learn the right action across all states. In these experiments, TOMA-VM constantly performs better than TOMA. The reason behind it is discussed in next section.

3.2.3 Dynamics

We visualize the trajectory and the generated graph during training on the Snake maze with sensor observation in Figure 6. We render the last 10 trajectories and the generated graph every 50 iterations. We find that TOMA will get stuck at the first corner simply because it fails to realize that it should go left, as the past experience from HER pool are mainly for going right and down. In contrast, since TOMA-VM can recall the past experience of reaching the middle of the second corridor, it can successfully go across the second corridor and reach the bottom.

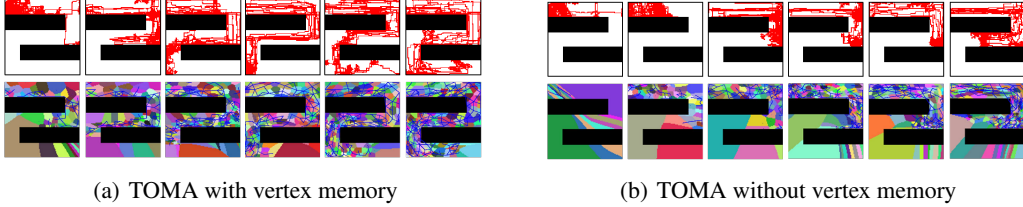


Figure 6: Last 10 trajectories and the generated graphs of TOMA-VM and TOMA every 50 iterations.

4 Related Work

Studies on animals [O’Keefe and Dostrovsky, 1971, Moser et al., 2008, Collett, 1996] reveal that animals are able to build an mental representation to reflect the topological map (graph) of the surrounding environment and animals will use such representation for navigation. This mental representation is usually termed as *mental map* [Lynch and for Urban Studies, 1960] or *cognitive map* [Tolman, 1948]. Furthermore, there exists evidence [Gillner and Mallot, 1998, Driscoll et al., 2000] showing that the mental representation is based on landmarks, which serve as an abstraction of the real environment.

Graph is a natural implementation of this mental representation. Inspired by this biological phenomenon, researchers have recently proposed to generate graph representation for RL. Existing methods such as SPTM [Savinov et al., 2018] and SoRB [Eysenbach et al., 2019] propose to generate graph representations for planning and they treat the states in the replay buffer as vertices. SPTM learns a reachability predictor and a locomotion model from random samples by self-supervised learning and it applies them over a replay buffer of human experience to compute paths towards goals. SoRB considers the value function of goal-conditioned policy as a distance metric, which is used to determine edges between vertices. SoRB requires to train the agent on several random generated goal reaching tasks in the environment during learning. Compared with these approaches which do not adopt abstraction, TOMA generates an abstract graph which has less memory and computation cost. Also, since TOMA is free from constraints such as human experience and training another RL agent, it can be used in RL exploration.

Graph generation methods are also related to some model-based RL methods [Sutton, 1990, Amos et al., 2018, Kaiser et al., 2020], but these model-based RL methods do not learn topological maps. There also exist some *state abstraction* methods like [Sutton et al., 1999, Singh et al., 1994, Andre and Russell, 2002, Mannor et al., 2004, Nouri and Littman, 2010, Li et al., 2006, Abel et al., 2016] for RL. But these state abstraction methods only aggregate states for abstraction but do not model topology information.

5 Conclusion

In this paper, we propose a novel graph generation method called TOMA for reinforcement learning, which can generate an abstract graph representation for MDP. TOMA costs much less memory and computation cost than existing methods. Furthermore, TOMA can be used for facilitating exploration. Experimental results show that TOMA can outperform existing methods to achieve the state-of-the-art performance. In the future, we will further explore other potential applications of TOMA.

6 Broader Impact

This work introduces a model learning algorithm for RL. Since the model learning approach is a common practice in RL and does not lead to any controversy, the proposed algorithm is not likely to pose ethical issues.

References

- J. O’Keefe and J. Dostrovsky. The hippocampus as a spatial map. preliminary evidence from unit activity in the freely-moving rat. *Brain Research*, 34(1):171 – 175, 1971.
- Edvard I. Moser, Emilio Kropff, and May-Britt Moser. Place cells, grid cells, and the brain’s spatial representation system. *Annual Review of Neuroscience*, 31(1):69–89, 2008.
- Edward C. Tolman. Cognitive maps in rats and men. *Psychological Review*, 55:189 – 208, 1948.
- Nikolay Savinov, Alexey Dosovitskiy, and Vladlen Koltun. Semi-parametric topological memory for navigation. In *Proceedings of the 6th International Conference on Learning Representations (ICLR)*, 2018.
- Ben Eysenbach, Ruslan Salakhutdinov, and Sergey Levine. Search on the replay buffer: Bridging planning and reinforcement learning. In *Proceedings of the Advances in Neural Information Processing Systems (NeurIPS)*, 2019.
- Xavier Glorot, Antoine Bordes, and Yoshua Bengio. Deep sparse rectifier neural networks. In *Proceedings of the 14th International Conference on Artificial Intelligence and Statistics (AISTATS)*, 2011.
- M.W. Hirsch. *Differential Topology*. Graduate Texts in Mathematics. Springer New York, 1997.
- Jon Louis Bentley. Multidimensional binary search trees used for associative searching. *Commun. ACM*, 18(9):509–517, 1975.
- Marcin Andrychowicz, Dwight Crow, Alex Ray, Jonas Schneider, Rachel Fong, Peter Welinder, Bob McGrew, Josh Tobin, Pieter Abbeel, and Wojciech Zaremba. Hindsight experience replay. In *Proceedings of the Advances in Neural Information Processing Systems (NeurIPS)*, 2017.
- Yann LeCun and Corinna Cortes. MNIST handwritten digit database. 2010.
- Diederik P. Kingma and Max Welling. Auto-encoding variational bayes. In *Proceedings of the 2nd International Conference on Learning Representations (ICLR)*, 2014.
- Volodymyr Mnih, Koray Kavukcuoglu, David Silver, Alex Graves, Ioannis Antonoglou, Daan Wierstra, and Martin Riedmiller. Human-level control through deep reinforcement learning. *Nature*, 518:529 – 533, 2015.
- Thomas Collett. Insect navigation en route to the goal: Multiple strategies for the use of landmarks. *The Journal of Experimental Biology*, 199:227–35, 02 1996.
- K. Lynch and Joint Center for Urban Studies. *The Image of the City*. Harvard-MIT Joint Center for Urban Studies Series. Harvard University Press, 1960.
- Sabine Gillner and Hanspeter Mallot. Navigation and acquisition of spatial knowledge in a virtual maze. *Journal of Cognitive Neuroscience*, 10:445–63, 08 1998.
- Ira Driscoll, Derek Hamilton, and Robert Sutherland. Limitations on the use of distal cues in virtual place learning. *Journal of Cognitive Neuroscience*, page 21, 01 2000.
- Richard S. Sutton. Integrated architectures for learning, planning, and reacting based on approximating dynamic programming. In *Proceedings of the 7th International Conference on Machine Learning (ICML)*, 1990.
- Brandon Amos, Ivan Dario Jimenez Rodriguez, Jacob Sacks, Byron Boots, and J. Zico Kolter. Differentiable MPC for end-to-end planning and control. In *Proceedings of the Advances in Neural Information Processing Systems (NeurIPS)*, 2018.

- Lukasz Kaiser, Mohammad Babaeizadeh, Piotr Milos, Blazej Osinski, Roy H Campbell, Konrad Czechowski, Dumitru Erhan, Chelsea Finn, Piotr Kozakowski, Sergey Levine, Afroz Mohiuddin, Ryan Sepassi, George Tucker, and Henryk Michalewski. Model-based reinforcement learning for Atari. In *Proceedings of the 8th International Conference on Learning Representations (ICLR)*, 2020.
- Richard S. Sutton, Doina Precup, and Satinder P. Singh. Between mdps and semi-mdps: A framework for temporal abstraction in reinforcement learning. *Artificial Intelligence*, 112(1-2):181–211, 1999.
- Satinder P. Singh, Tommi S. Jaakkola, and Michael I. Jordan. Reinforcement learning with soft state aggregation. In *Proceedings of the Advances in Neural Information Processing Systems (NeurIPS)*, 1994.
- David Andre and Stuart J. Russell. State abstraction for programmable reinforcement learning agents. In *Proceedings of the 18th National Conference on Artificial Intelligence and the 14th Conference on Innovative Applications of Artificial Intelligence (AAAI)*, 2002.
- Shie Mannor, Ishai Menache, Amit Hoze, and Uri Klein. Dynamic abstraction in reinforcement learning via clustering. In *Proceedings of the 21st International Conference on Machine Learning (ICML)*, 2004.
- Ali Nouri and Michael L. Littman. Dimension reduction and its application to model-based exploration in continuous spaces. *Machine Learning*, 81(1):85–98, 2010.
- Lihong Li, Thomas J. Walsh, and Michael L. Littman. Towards a unified theory of state abstraction for mdps. In *Proceedings of the 9th International Symposium on Artificial Intelligence and Mathematics (ISAIM)*, 2006.
- David Abel, D. Ellis Hershkowitz, and Michael L. Littman. Near optimal behavior via approximate state abstraction. In *Proceedings of the 33rd International Conference on Machine Learning (ICML)*, 2016.
- Diederik P. Kingma and Jimmy Ba. Adam: A method for stochastic optimization. In *Proceedings of 3rd International Conference on Learning Representations, ICLR*, 2015.
- Laurens van der Maaten and Geoffrey Hinton. Visualizing data using t-SNE. *Journal of Machine Learning Research*, 9:2579–2605, 2008.

Appendix

A Experiment Details

A.1 Environment

The 2D worlds used in the experiment are all 100×100 grid spaces. The sensor observation is normalized to $[-1, 1]$ before feeding to the agent. The size of MNIST digit observation is 25×25 and the size of top-down observation is 50×50 . The pixel value of MNIST digit and top-down observations are also normalized to $[-1, 1]$.

We use following approach to generate MNIST digits instead of using generative models. First, we choose n different MNIST digit images from the dataset, denoted as $\{o_1, o_2, \dots, o_n\}$. Then we assign each x_i with a center location $(x_i, y_i) \in [0, 99] \times [0, 99]$. Then for agent at location $(x, y) \in [0, 99] \times [0, 99]$, we generate the observation o using a weighted sum

$$o = \frac{\sum_{i=1}^n w_i o_i}{\sum_{i=1}^n w_i},$$

where

$$w_i = \exp(-0.01 \sqrt{(x - x_i)^2 + (y - y_i)^2}).$$

In the experiments, we randomly select 4 different MNIST digit images and place them at (10, 10), (10, 90), (90, 10) and (90, 90) respectively.

A.2 Embedding Network

The embedding networks used in the experiments are shown in Table 2, Table 3 and Table 4. In the table, ‘FC’ stands for fully connected layer and ‘Conv’ stands for convolution layer. We train these networks using Adam optimizer Kingma and Ba [2015] with learning rate 0.0001, $\beta = (0.9, 0.999)$. We draw samples uniformly from a replay pool of size 100k. In each iteration, we update this replay pool with 400 samples. The batch size is 64. The size of ensemble used in top-down maze is 8. In planning experiment, r is set to 20. In exploration experiment, r is set to 8.

A.3 Goal-conditioned Agent

The goal-conditioned agent used in the planning experiment is the locomotion network proposed in SPTM Savinov et al. [2018]. The locomotion networks used in planning experiments are shown in Table 5, Table 6 and Table 7.

A.4 Q-network

The Q-networks used in the experiments are shown in Table 8, Table 9, Table 10 and Table 11. We set the discount factor $\gamma = 0.95$, ϵ -greedy factor $\epsilon = 0.9$ in all the exploration experiments. We train these networks using Adam optimizer with learning rate 0.0003, $\beta = (0.9, 0.999)$. The batch size is 256. The size of HER is 100k. The goal number k of HER is set to 4 in MountainCar experiments and is set to 16 in Snake maze experiments. The memory pool of each vertex holds at most 1k samples. For better exploration, the DQN agent chooses action randomly after $0.9T$ steps in each iteration, where T is the total steps of each iteration.

A.5 Planning

Since our graph is an abstraction of environment, it’s not necessary to plan at each step. Instead, we carry out planning every 10 steps in planning experiments and exploration experiments.

B Further Analysis

B.1 Effect of r

We measure the effect of radius r and find it is consistent with our expectation. We use “Empty” map and let $r = 8, 16, 32$ for different levels of abstraction. The graph generation results are illustrated in

Figure 7 (b). The state coverage of each vertex does increase as we increase r , leading to a higher level of abstraction.

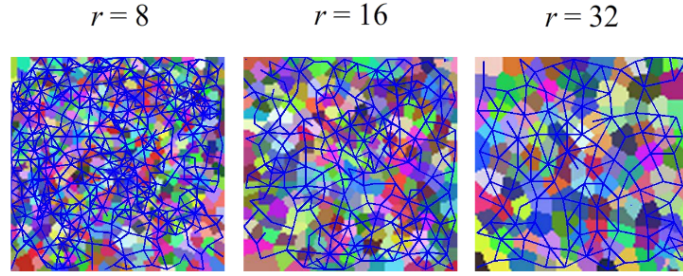


Figure 7: Effect of r .

B.2 Visualizing Embedding Space

We use t-SNE [van der Maaten and Hinton, 2008] to visualize the embedding space of the sensor and MNIST digit maze on the plane. The result is shown in Figure 8. Though only exposed to visual features, TOMA still successfully captures the underlying topological map of the world.

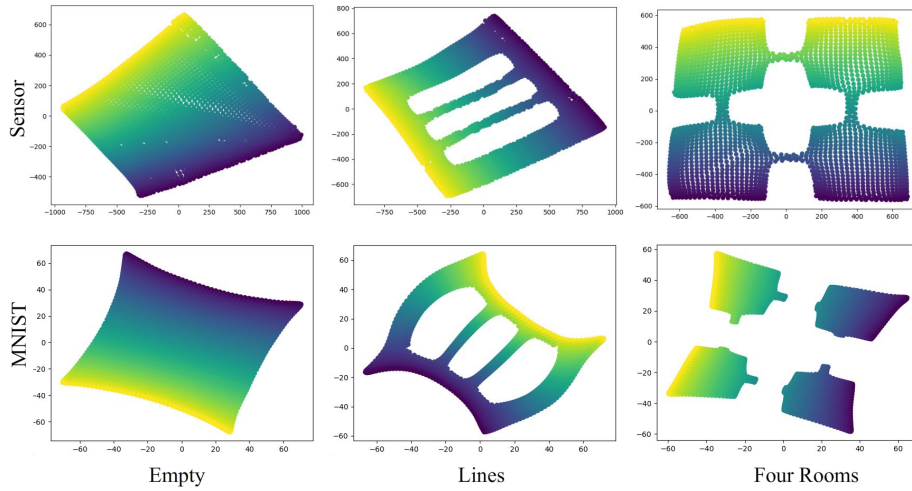


Figure 8: Visualization of embedding space.

Table 2: Embedding network for sensor maze and MountainCar.

FC 64, ReLU
FC 64, ReLU
FC 8

Table 3: Embedding network for MNIST digit maze.

Conv 6x6, channel 16, stride 2, ReLU
Conv 6x6, channel 16, stride 2, ReLU
Conv 3x3, channel 16, stride 2, ReLU, flatten to 256
FC 64, ReLU
FC 8

Table 4: Embedding network for top-down maze.

Conv 5x5, channel 64, stride 4, ReLU
Conv 3x3, channel 128, stride 2, ReLU
Conv 3x3, channel 128, stride 2, ReLU
Conv 3x3, channel 128, stride 1, ReLU, flatten to 2048
FC 8

Table 5: Locomotion network for sensor maze.

FC 16, ReLU
Concatenate two encoded vectors.
FC 32, ReLU
FC 32, ReLU
FC 4

Table 6: Locomotion network for MNIST digit maze.

Conv 4x4, channel 32, stride 2, ReLU
Conv 4x4, channel 32, stride 2, ReLU
Conv 4x4, channel 32, stride 2, ReLU, flatten to 512
Concatenate two encoded vectors.
FC 512, ReLU
FC 512, ReLU
FC 4

Table 7: Locomotion network for top-down maze.

Conv 5x5, channel 64, stride 4, ReLU
Conv 3x3, channel 64, stride 2, ReLU
Conv 3x3, channel 64, stride 2, ReLU
Conv 3x3, channel 64, stride 1, ReLU, flatten to 1024
Concatenate two encoded vectors.
FC 512, ReLU
FC 512, ReLU
FC 4

Table 8: Q-network for MountainCar.

FC 64, ReLU
FC 64, ReLU
FC 3

Table 9: Q-network for sensor maze.

FC 300, ReLU
FC 200, ReLU
FC 4

Table 10: Q-network for MNIST digit maze.

Conv 6x6, channel 32, stride 4, ReLU
Conv 4x4, channel 64, stride 2, ReLU
Conv 4x4, channel 64, stride 1, ReLU, flatten to 1024
FC 256, ReLU
FC 4

Table 11: Q-network for top-down maze.

Conv 6x6, channel 64, stride 4, ReLU
Conv 4x4, channel 128, stride 2, ReLU
Conv 4x4, channel 128, stride 2, ReLU, flatten to 2048
FC 512, ReLU
FC 4